JOURNAL OF THEORETICAL
AND APPLIED MECHANICS
63, 1, pp. 165-175, Warsaw 2025
https://doi.org/10.15632/jtam-pl/196983

EFFECT OF MATERIAL PARAMETERS ON THE CUMULATIVE FATIGUE DAMAGE OF SONIC OSCILLATORS

Shengyu He, Changgen Bu, Xiuhua Zheng, Jing Xiao, Xiangzhou Kong
School of Engineering and Technology, China University of Geosciences, Beijing, China
corresponding author Changgen Bu, e-mail: bucg@cugb.edu.cn

The standing-wave vibration drill-string in a sonic drill is prone to fatigue damage. Commonly used alloy materials for drill-strings include S135, 4145H and G105, but the material sensitivity coefficient is large when the fatigue strength is high. To choose an appropriate drill-pipe material and improve the drill-string service life, this paper analyzes the cumulative fatigue damage of three types of material drill-strings with variable length. The results indicate that for short drill-strings with high-frequency vibrations, the material constant has a greater effect on fatigue damage. However, for long drill-strings with low-frequency vibrations, the fatigue limit has a greater impact on fatigue damage.

Keywords: sonic oscillators, sonic drilling, cumulative fatigue damage, standing wave vibration, material parameters

Nomenclature

c – damping coefficient
d_i, d_o – inner and outer diameter of drill string, respectively
$f(x,t)$ – distributed load
k – number of additional drill pipes
k_{max} – total number of additional drill pipes within fatigue damage zone
l – length of drill string
l_b – length of drill string without fatigue damage
l_0 – maximum drill string length before entering standing wave vibration
m – material constant
m_e – static moment of sonic vibrator
m_H, m_G, m_S – material constant of 4145H, G105, S135, respectively
n_k – number of cycles under stress level σ_{-1k}
$u(x,t)$ – displacement response of drill string
x_f – distance from any point on drill string to drill bit
D – cumulative fatigue damage
D_H, D_G, D_S – fatigue damage of 4145H, G105, S135, respectively
E – elastic modulus
N_C, N_k – total number of cycles under stress level σ_{-1} and σ_{-1k}, respectively
R_{HG}, R_{SG} – damage ratio at maximum damage point of 4145H and G105; S135 and G105, respectively
S – cross-sectional area of drill string
V – rate of penetration (ROP)
Δl – length of single drill pipe

ζ – damping ratio
ρ – density
$\varepsilon(x,t), \sigma(x,t)$ – dynamic strain and stress, respectively
σ_b – tensile strength
σ_{-1} – symmetrical cyclic fatigue limit stress
σ_{-1k} – stress level
φ_i – phase angle
ω_i – i-th order natural angular frequency

1. Introduction

In the context of geological and oil drilling operations, a drill tool is subjected to tension, bending, torsion, impact, and hydraulic pressure in the wellbore. These complex stress conditions are a primary cause of fatigue failure in drill strings (Albdiry and Almensory, 2016). Research has shown that over 50% of drill-string failures are caused by fatigue (Moradi and Ranjbar, 2009). Constant axial, torsional, and internal pressure loads do not cause fatigue, but they can exacerbate fatigue under the influence of cyclic stress (Asgharzadeh *et al.*, 2019). Drill strings fatigue damage is a major concern for researchers worldwide.

Recently, sonic (or ultrasonic) vibration technology has rapidly developed and been applied in the field of drilling. Sonic (ultrasonic) drilling is an efficient drilling method that utilises resonant waves in a drill string to generate higher speeds in the drill bit, thereby achieving high-speed drilling. It has the advantages of high drilling speed, high fidelity of rock samples, and low environmental pollution and is widely used in fields such as engineering exploration and infrastructure construction. However, the standing wave resonance in drill strings can cause extreme dynamic stresses at specific locations within the drill string, which can lead to fatigue failure or even fracture of the drill string, increasing drilling costs (Zamani *et al.*, 2016).

Fatigue failure is the process of fatigue damage accumulation reaching a critical value. Numerous theoretical models have been developed to describe the development of cumulative damage (Benkabouche *et al.*, 2015). In engineering applications, the Miner cumulative fatigue damage theory is notable for its simplicity and practical utility. It often aligns well with experimental results and is adept at predicting the average fatigue life of engineering structures under random loads (Sun *et al.*, 2014). This theory is widely applied in predicting the fatigue life of various mechanical components in engineering, such as aircraft engines, skin, and hydraulic tubes and other components (Baek *et al.*, 2008; Chen *et al.*, 2014; Jiao *et al.*, 2018). Rao *et al.* (2001) reported that the Palmgren–Miner law is the most used theory for predicting the fatigue life in blades subjected to variable stress amplitudes. Zhao *et al.* (2018) employed the rainflow-counting method to analyze continuous bending stress history in whirl responses, and evaluated the cumulative fatigue damage using Miner's rule. Additionally, Zhu *et al.* (2012) indicated that the Palmgren–Miner rule provides a better lifetime prediction under simple loading conditions, as compared to other methods. Bu *et al.* (2023) theoretically investigated the fatigue damage in sonic drilling caused by inertial excitation, and conducted a fatigue damage theory for deep-hole sonic drilling by using Miner's cumulative fatigue damage rule.

Research on fatigue experiments has mainly focused on fatigue damage analyzes of material samples. The metal magnetic memory method can be employed to quantitatively assess material damage based on the characteristics of metal magnetic memory changes during stress or fatigue of different materials. Many studies have been conducted on the processes of tensile fatigue and rotary-bending fatigue (Li *et al.*, 2013, 2016). Lin *et al.* (2015) conducted fatigue performance tests on commonly used API standard S135 and G105 materials by employing a PQ-6 rotary-bending fatigue-testing machine. By utilizing the Basquin model and mathematical statistics theory, Lin obtained the S-N curves for these materials. Wang *et al.* (2016) using the same method as Lin *et al.* (2015), obtained the S-N curves for 4145H, 4145H is international standard drilling tool steel certified by the American Iron and Steel Institute (AISI). Furthermore, it was found that the frequency of ultrasonic testing did not impact the fatigue life in tests of asymmetric cyclic loads with constant- and variable-amplitude loads (Mayer *et al.*, 2013; Fitzka and Mayer, 2016). Experimental studies on material fatigue damage have only focused on a specific load. However, during sonic drilling, as the borehole extends, the excitation frequency decreases, and the location of the maximum dynamic stress changes. Therefore, the dynamic stress experienced by each point in the drill string is different, and each point in the drill string is subjected to varying amplitude loads (Bu *et al.*, 2015). Therefore, fatigue damage analysis and research on resonant drill strings in sonic drilling should not only focus on the material itself but also be combined with the actual working conditions.

In our previous research, we developed a theory on fatigue damage of sonic drill strings, which theoretically proved the primary role of resonant order stress in causing fatigue damage, and our findings suggested that selecting materials with a high fatigue limit and low material constant (index of σ-N curve) can reduce the damage of drill strings (Bu *et al.*, 2023). However, the influence of materials on the fatigue life was not theoretically analyzed and the fatigue life of different materials under the same stress cycle was not evaluated; thus, whether a larger fatigue limit leads to a longer fatigue life is still unknown. Compared to G105 materials, S135 materials have a higher fatigue limit and a higher material constant, which is more sensitive to the stress cycle. The material constant and fatigue limit of 4145H material are both between S135 and G105. Therefore, during construction, both the fatigue limit and the material constant should be considered. For shallow sonic drills using piezoelectric ceramics or giant magnetostrictive materials as exciters (Bu *et al.*, 2022) or ultrasonic knives used in the medical field, the excitation frequency is high (up to 20–100 kHz). In such cases, considering the impact of material constants on the fatigue life is crucial.

This study compares the fatigue damage of S135, 4145H and G105 drill strings, which are commonly used in drilling projects, by applying the Miner cumulative fatigue damage rule combined with the standing-wave vibration characteristics of sonic drilling. Furthermore, the fatigue damage of three types of drill strings having the same length is analyzed, and the application range of the three materials is determined. This study is important for guiding engineering practices on choosing appropriate drill pipe materials, reducing drilling accidents and enhance the service life of sonic drill strings.

2. Methodology

2.1. Stress analysis of sonic drill string

In sonic drilling, a sonic vibrator is installed at the top of the drill to induce vibrations in the drill string. This vibrator is isolated using air springs, ensuring it does not participate to the resonance of the drill string (Xiao *et al.*, 2020). According to our previous work (Bu *et al.*, 2023), the differential equation to describe the longitudinal vibration of a sonic drill string is

$$\rho S\frac{\partial^2 u}{\partial t^2} + c\frac{\partial u}{\partial t} - ES\frac{\partial^2 u}{\partial x^2} = f(x,t) \tag{2.1}$$

where ρ is the material density, S is the cross-sectional area of the drill string, c is the damping coefficient, E is the elastic modulus, and $f(x,t) = m_e\omega^2\sin(\omega t)\delta(x)$, $\delta(x)$ is the Dirac delta function, $\int_0^l f(x,t)\,dx = m_e\omega^2\sin(\omega t)$, m_e is the static moment of the sonic vibrator.

The boundary condition is expressed as

$$\frac{\partial u(0,t)}{\partial x} = \frac{\partial u(l,t)}{\partial x} = 0 \tag{2.2}$$

The vibration differential equation and boundary conditions of the sonic drill string are obtained by applying Eqs. (2.1) and (2.2), and the steady-state solution of the forced vibration displacement response of the drill string is obtained by using the separated variable method (Sun *et al.*, 2017)

$$u(x,t) = \frac{2m_e\omega^2}{\rho Sl}\sum_{i=0}^{\infty}\frac{\sin\omega\,t-\varphi_i}{\sqrt{(\omega_i^2-\omega^2)^2+(2\zeta_i\omega_i\omega)^2}}\cos\frac{i\pi x}{l} \tag{2.3}$$

where $\omega_i = (i\pi/l)\sqrt{(E/\rho)}$ $(i = 1,2,3,...)$ is the natural angular frequency, $\varphi_i = \arctan((2\zeta_i\omega_i\omega)/(\omega_i^2-\omega^2))$ is the phase angle, and ζ_i is the mode shape damping ratio (it is usually assumed that the damping ratio of each mode is the same; therefore, $\zeta_i = \zeta$). When the excitation angular frequency ω approaches ω_i, the phase angle φ_i approaches $\pi/2$.

Then, the stress expression can be obtained as follows

$$\sigma(x,t) = E\varepsilon(x,t) = E\frac{\partial u(x,t)}{\partial x} = -\frac{2\pi Em_e\omega^2}{\rho Sl^2}\sum_{i=0}^{\infty}\frac{i\sin\omega t-\varphi_i}{\sqrt{(\omega_i^2-\omega^2)^2+(2\zeta_i\omega_i\omega)^2}}\sin\frac{i\pi x}{l} \tag{2.4}$$

The material parameters of S135, 4145H and G105 drill pipes are listed in Table 1.

Table 1. Material parameters of drill pipes (Lin *et al.*, 2015; Wang *et al.*, 2016)

Drill pipe material	Fatigue limit σ_{-1} [MPa]	Tensile strength σ_b [MPa]	Material constant m	Density ρ [kg/m^3]	Elastic modulus E [Pa]
S135	527.37	1000	16.53	7850	2.06e11
4145H	482.89	1100	12.81	7850	2.06e11
G105	435.62	793	9.77	7850	2.06e11

The technical parameters of the sonic vibrator and drill pipe are presented in Table 2.

Table 2. Technical parameters of the sonic vibrator and drill pipe (Sun *et al.*, 2017; Bu *et al.*, 2023)

Total static moment of sonic vibrator m_e	Drill-string inner/outer diameter d_i/d_o	Drill-string cross-sectional area S
0.126 kg · m	92.46/114.3 mm	3.547e-3 m^2

Table 1 indicates that the three materials have the same density and elastic modulus. Then, according to Eq. (2.4), the dynamic stress produced by standing wave vibration is the same for drill strings having the same length. We can determine the relationship between the maximum dynamic stress amplitude of the first-order resonant sonic drill string and its length by substituting the technical parameters listed in Table 2 into Eq. (2.4), as shown in Fig. 1.

Figure 1 illustrates that as the length of the drill string increases, its maximum dynamic stress amplitude gradually decreases, and the peak dynamic stress of the first-order resonance is always located in the middle of the drill string. Fatigue damage occurs when the dynamic stress amplitude of the drill string exceeds the fatigue limit. Due to the highest fatigue limit of the S135 material, the S135 drill pipe enters the non-damage zone earliest with the extension of the drill string.

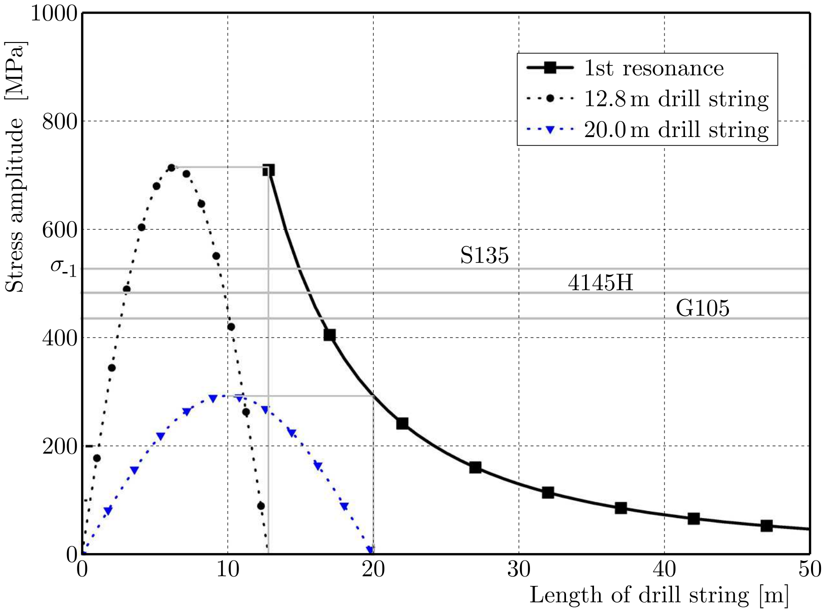

Fig. 1. Maximum stress amplitude of sonic drill strings having different lengths. The black dashed line represents the dynamic stress amplitude at each point of the 12.8 m drill string, and the blue dashed line represents the dynamic stress amplitude at each point of the 20 m drill string

2.2. Cumulative fatigue damage of the sonic drill string

When the influence of various dynamic stresses in the drill string on the fatigue life is analyzed, the fatigue damage of the drill string can be considered caused by the resonant dynamic stress. According to Miner's cumulative fatigue damage theory, $D = \sum(n_k/N_k)$, where n_k is the number of cycles under the stress level σ_{-1k} $(k = 1, 2, 3, ...)$, N_k is the total number of cycles that the test piece can withstand under the stress level σ_{-1k}, and the fatigue damage expression for the drill string (Bu *et al.*, 2023) can be obtained as

$$D = \frac{\pi^m r^{m+1}}{2N_C(\sigma_{-1})^m}\Big(\sqrt{\frac{E}{\rho}}\Big)^{2m+1}\Big(\frac{m_e}{S}\Big)^m \frac{1}{V\zeta^m}\sum_{k=1}^{k_{max}}\Big[\frac{\Delta l}{(l_0+k\Delta l)^{2m+1}}\sin^m\Big(\frac{\pi x_f}{l_0+k\Delta l}\Big)\Big] \tag{2.5}$$

where V is the rate of penetration (ROP), σ_{-1} is the symmetrical cyclic fatigue limit, N_C is the total number of cycles under the stress level σ_{-1}, m is the material constant, x_f is the distance from any point on the drill string to the drill bit, l_0 is the maximum length of the drill string before entering the standing wave vibration, Δl is the length of a single drill pipe, k is the number of additional drill pipes, and k_{max} is the total number of additional drill pipes within the fatigue damage zone, which is affected by the excitation frequency and the material fatigue limit.

As shown in Table 1, the S135, 4145H and G105 materials have the same elastic modulus and density. Therefore, based on Eq. (2.5), the factors affecting the damage between the two materials are the material fatigue limit and the material constant. The two parameters have opposite effects on the fatigue damage, with a high fatigue limit resulting in low fatigue damage, and a high material constant resulting in high fatigue damage. Table 1 reveals that the S135 material has the highest fatigue limit and highest material constant; so, the S135 material is most sensitive to stress cycles. Therefore, drill-string materials should be selected for more specific operating conditions to obtain a longer fatigue life.

3. Results and discussion

According to the foregoing analysis, the total cumulative fatigue damage during the drilling process was obtained based on the stress cycle times and fatigue life of the drill string at different stress levels. In this Section, the cumulative fatigue damage of the drill string for all materials listed in Table 1 are compared by setting continuous drilling conditions under different excitation frequencies. Additionally, the damage ratios of the fixed-length drill string oscillator are analyzed at different frequencies to explore the effects of the material fatigue limit and material constants on damage.

3.1. Fatigue damage comparison of variable-length sonic drilling

In sonic drilling, the extension of the drill string leads to a continuous change in force distribution. The static moment of the sonic vibrator and geometric parameters of the drill string are shown in Table 2, and the working conditions (damping ratio $\zeta = 0.025$ and ROP $= 15\,\mathrm{m/h}$) are set. Based on setting the length of a single drill pipe to $\Delta l = 0.1\,\mathrm{m}$ (equivalent to the continuous extension of the drill string), the fatigue damages of S135, 4145H and G105 drill strings due to the standing wave resonance at initial excitation frequencies of 180 and 206 Hz are calculated.

When the initial excitation frequency is 180 Hz, the sonic standing wave begins at a drill string length of 14.2 m. Figure 2 shows the cumulative fatigue damages of the S135, 4145H and G105 drill strings as the drilling proceeded until no further fatigue damage occurred.

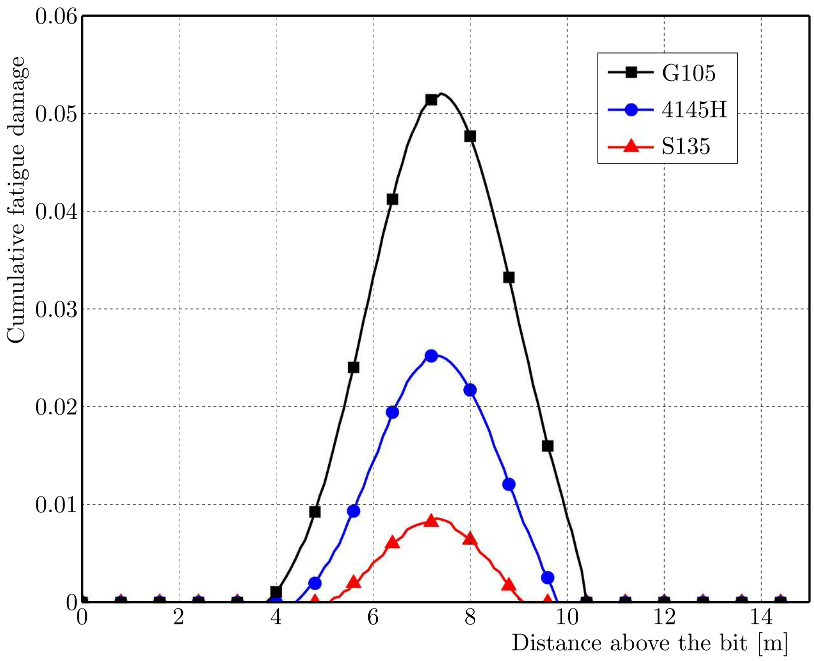

Fig. 2. At the initial excitation frequency of 180 Hz, the starting length of the sonic standing wave is 14.2 m; drilling is performed to the point where fatigue damage no longer occurs, and the cumulative fatigue damages at various points of S135, 4145H and G105 drill strings are shown (drilling conditions: $\zeta = 0.025$, $\Delta l = 0.1\,\mathrm{m}$, and ROP $= 15\,\mathrm{m/h}$)

Figure 2 shows that the S135 drill pipe, which has the highest fatigue limit, has lowest damage at all points; the G105 drill pipe, which has the lowest fatigue limit, has highest damage at all points; the fatigue limit and the fatigue damage of 4145H drill pipe are both between G105 and S135.

This result supports the idea that the higher the material fatigue limit, the lower the fatigue damage and the longer the lifespan. When the maximum dynamic stress amplitude of the drill string reaches the fatigue limits of S135, 4145H and G105, respectively, the specific excitation frequencies determined by Eq. (2.4) are 171.9 Hz, 164.5 Hz and 156.2 Hz, respectively. Notably, if the initial excitation frequency is lower than 156.2 Hz, the maximum dynamic stresses of these three materials are less than the fatigue limits, and none of them will experience fatigue damage. Therefore, these three materials can be selected.

In the case of long drill string at low frequencies, materials with a high fatigue limit exhibit low fatigue damage. However, for shallow sonic standing-wave drilling or drilling with a shorter drill string, the drilling string has a higher excitation frequency and undergoes more stress cycles per unit time. According to the data in Table 1, S135 material with the highest fatigue limit has the same highest material constant and is most sensitive to dynamic stress cycling. Therefore, the use of S135 for high-frequency short drill strings requires further investigation.

The starting length of the sonic standing wave is 12.4 m when the initial excitation frequency increases to 206 Hz. Drilling is performed to the point where fatigue damage no longer occurs, and the cumulative fatigue damages of the S135, 4145H and G105 drill strings are shown in Fig. 3.

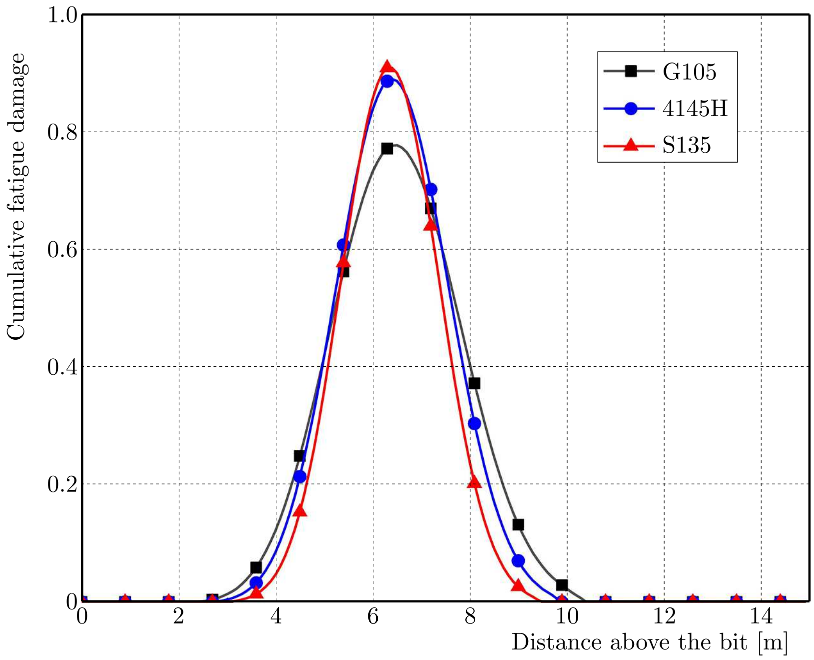

Fig. 3. At the initial excitation frequency of 206 Hz, the starting length of the sonic standing wave is 12.4 m; drilling is performed to the point where fatigue damage no longer occurs, and the cumulative fatigue damages at various points of S135, 4145H and G105 drill strings are shown (drilling conditions: $\zeta = 0.025$, $\Delta l = 0.1$ m, and ROP $= 15$ m/h)

As shown in Fig. 3, the maximum damage points of these three materials are near the distance from the drill bit of half the starting length of the sonic standing wave. The maximum cumulative fatigue damage of S135 is the highest, while the maximum cumulative fatigue damage of G105 is the lowest, and the maximum cumulative fatigue damage of 4145H is between G105 and S135. This result is inconsistent with the conclusion drawn from Fig. 2. If the starting length of the sonic standing wave decreases and the standing-wave excitation frequency increases, the fatigue damage to the S135 drill string becomes greater, potentially leading to its failure. This is because fatigue damage is not only related to the fatigue limit but also significantly influenced by the material constant. The higher-frequency excitation causes the dynamic stresses in the symmetric cycle in the drill string to change faster, and the S135 material has the highest constant and is most sensitive to stress changes; therefore, the maximum damage is highest in these three materials.

A comparison of the two types of special cases presented in Figs. 2 and 3 reveal that when drilling with a low-frequency and long drill string, the greater the fatigue limit, the smaller is the fatigue damage; when drilling with high-frequency short drill strings, the smaller the material coefficient, the smaller is the fatigue damage. This also indicates that under different excitation frequencies, the fatigue limit and material constant have different dominant effects on the fatigue life of the drill strings. Therefore, it is not feasible to evaluate the cumulative fatigue damage of the drill string based on a single parameter only, and a combination of fatigue limits and material constants needs to be considered.

3.2. Effect of standing wave oscillator length on the fatigue damage ratio of two materials

In contrast to the special case analysis of the standing-wave vibration drill string previously described, a more general case is discussed. The theory of cumulative fatigue damage means that when the dynamic stress is below the fatigue limit of the material, damage will no longer occur (Miner, 1945). According to our previous study, the excitation frequency and dynamic stress gradually decrease when the length of the drill string varies from short to long (Bu *et al.*, 2023). The formula for calculating the length of drill-string for which the standing wave resonance no longer causes fatigue damage is

$$l_b = \sqrt{\frac{\pi r m_e}{\zeta \sigma_{-1} S}} \sqrt{\frac{E}{\rho}} \tag{3.1}$$

The lengths of the three drill strings without fatigue damage are obtained as 14.9 m, 15.6 m and 16.4 m by substituting the material parameters of S135, 4145H and G105 presented in Table 1 into Eq. (3.1). Therefore, the analysis should be performed when the length of the drill-string oscillator is less than 14.9 m.

A fixed length of the drill string oscillator is set to analyze the fatigue damage of the three materials. To compare the extent of damage to the three materials more intuitively, the material parameters of S135, 4145H and G105 are introduced into Eq. (2.5), and the fatigue damage of the three materials can be obtained as D_S, D_H and D_G; therefore, taking D_G as the denominator, D_S and D_H as the numerators, the damage ratios can be obtained as

$$\begin{aligned} \frac{D_S}{D_G} &= \Big(\frac{\pi r m_e E}{\zeta \rho S l^2} \sin\Big(\frac{\pi x_f}{l}\Big)\Big)^{m_S - m_G} \frac{(\sigma_{-1G})^{m_G}}{(\sigma_{-1S})^{m_S}} \\ \frac{D_H}{D_G} &= \Big(\frac{\pi r m_e E}{\zeta \rho S l^2} \sin\Big(\frac{\pi x_f}{l}\Big)\Big)^{m_H - m_G} \frac{(\sigma_{-1G})^{m_G}}{(\sigma_{-1H})^{m_H}} \end{aligned} \tag{3.2}$$

where subscripts S, H and G represent the S135, 4145H and G105 materials, respectively. When $\sin(\pi x_f/l) = 1$, the damage ratios at the maximum damage point of drill strings are obtained as

$$\begin{aligned} R_{SG} &= \frac{D_{S\,max}}{D_{G\,max}} = \Big(\frac{\pi r m_e E}{\zeta \rho S l^2}\Big)^{m_S - m_G} \frac{(\sigma_{-1G})^{m_G}}{(\sigma_{-1S})^{m_S}} \\ R_{HG} &= \frac{D_{H\,max}}{D_{G\,max}} = \Big(\frac{\pi r m_e E}{\zeta \rho S l^2}\Big)^{m_H - m_G} \frac{(\sigma_{-1G})^{m_G}}{(\sigma_{-1H})^{m_H}} \end{aligned} \tag{3.3}$$

For the three materials under the same working conditions, all the parameters in Eqs. $(3.3)_1$ and $(3.3)_2$ are the same, except for the material constant, m, and the fatigue limit, σ_{-1}, with only one variable, l. Therefore, the damage ratios are a function of the drill-string oscillator length, l.

The functional relationship between the fatigue damage ratio at the maximum damage points of the three drill strings and the oscillator length can be obtained by substituting the parameters in Table 2 into Eqs. $(3.3)_1$ and $(3.3)_2$, as shown in Fig. 4.

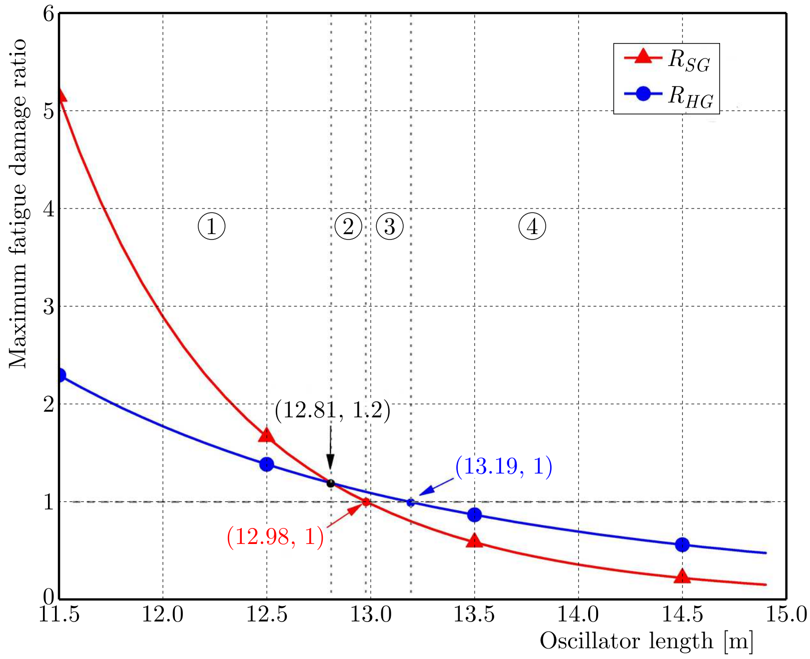

Fig. 4. Relationship between the length of the drill-string standing-wave oscillator and the maximum fatigue ratios; the damping ratio is set to 0.025

Figure 4 depicts that as the oscillator length increases, the damage ratio R_{SG} (red curve) decreases more sharply than R_{HG} (blue curve). Because the materials fatigue limit and material constant are fixed values, when the oscillator length l increases, $1/l^2$ becomes smaller, and the damage ratios R_{SG} and R_{HG} are proportional to $(1/l^2)^{m_S-m_G}$ and $(1/l^2)^{m_H-m_G}$, respectively. Meanwhile $m_S - m_G > m_H - m_G > 1$, thus R_{SG} decreases more sharply than R_{HG}.

As the oscillator length varies, the relationship between the maximum fatigue damage of these three materials also changes. According to Eqs. $(3.3)_1$ and $(3.3)_2$, when $D_{S\,max} = D_{H\,max}$, the damage ratio $R_{SG} = R_{HG} = 1.2$, $l = 12.81$ m. Define $l \leqslant 12.81$ m as the region ① (shown in Fig. 4) where $R_{SG} \geqslant R_{HG} > 1$ (i.e. $D_{G\,max} < D_{H\,max} \leqslant D_{S\,max}$). When $R_{SG} = 1$ or $R_{HG} = 1$, $l = 12.98$ m or $l = 13.19$ m; with $l = 12.98$ m and $l = 13.19$ m as regions boundaries, define regions ② $12.81\,\text{m} < l \leqslant 12.98\,\text{m}$, ③ $12.98\,\text{m} < l \leqslant 13.19\,\text{m}$, and ④ $13.19\,\text{m} < l < 14.90\,\text{m}$. The relationships between the maximum fatigue damage of materials in all four regions ①, ②, ③ and ④ can be summarized as

$$
\begin{array}{ll}
① : D_{G\,max} < D_{H\,max} \leqslant D_{S\,max} & l \leqslant 12.81\,\text{m} \\
② : D_{G\,max} \leqslant D_{S\,max} < D_{H\,max} & 12.81\,\text{m} < l \leqslant 12.98\,\text{m} \\
② : D_{S\,max} < D_{G\,max} \leqslant D_{H\,max} & 12.98\,\text{m} < l \leqslant 13.19\,\text{m} \\
④ : D_{S\,max} < D_{H\,max} < D_{G\,max} & 13.19\,\text{m} < l < 14.90\,\text{m}
\end{array}
\tag{3.4}
$$

From Eq. (3.4), it can be seen that the G105 oscillator experiences the lowest damage when the oscillator length is less than 12.98 m. Therefore, for a shallow high-frequency sonic drilling under piezoelectric ceramic or giant magnetostrictive excitation, materials with low material constants should be selected to reduce their sensitivity to stress changes and fatigue damage. However, the S135 oscillator experiences the lowest damage when the oscillator length is greater than 12.98 m. Therefore, for long drill strings with a low-frequency excitation, materials with a high fatigue limit should be selected to extend the fatigue life of the drill string.

The best case for selecting drill string materials is when the material has both a high fatigue limit and a small material constant, such that the standing-wave vibration drill string can have a high fatigue life in both high- and low-frequency operating ranges. However, the cost of these materials must be considered in engineering applications. In the case of commonly used alloy materials, simultaneously satisfying these two conditions is challenging. Therefore, an appropriate drill pipe material must be selected depending on different construction conditions.

4. Conclusions

Based on the Miner cumulative fatigue damage theory combined with the characteristics of a standing-wave vibration sonic drill string under variable frequency and amplitude dynamic stress, the fatigue damage of S135, 4145H and G105 materials commonly used in drilling construction is compared, and the following conclusions are drawn.

When the impact of materials on damage is examined, analyzing only a single material parameter is not sufficient. The fatigue limit and material constant must be comprehensively considered, and the length of the drill string and the excitation frequency influence the material selection. As the drill-string length increases, the frequency of the standing wave excitation decreases, the effect of the material constant on the fatigue damage gradually diminishes, and the impact of the fatigue limit on fatigue damage increases. For high-frequency short drill strings (oscillators), drill pipes with low material constants should be selected to reduce drill-string fatigue damage. For low-frequency long drill strings (oscillators), drill pipes with a high fatigue limit should be selected to reduce fatigue damage. This conclusion provides a practical value and theoretical guidance for selection of drill pipe materials in production.

Acknowledgements

This work was supported by the National Natural Science Foundation of China (Grant No. 51775523), Science and Technology Innovation Special Project of Xiongan New Area, Ministry of Science and Technology of the People's Republic of China (No. 2022XAGG0500).

References

1. Albdiry M.T., Almensory M.F., 2016, Failure analysis of drillstring in petroleum industry: A review, *Engineering Failure Analysis*, **65**, 74-85

2. Asgharzadeh A., Meza O.G., Bannenberg M., Paz C., Holzmann J., Oppelt J., 2019, New concept for multiaxial fatigue rigs in reconstructing combined loads to investigate fatigue life of casing connections in casing drilling applications, *Offshore Mediterranean Conference and Exhibition*, OMC-2019-0856

3. Baek S.H., Cho S.S., Joo W.S., 2008, Fatigue life prediction based on the rainflow cycle counting method for the end beam of a freight car bogie, *International Journal of Automotive Technology*, **9**, 1, 95-101

4. Benkabouche S., Guechichi H., Amrouche A., Benkhettab M., 2015, A modified nonlinear fatigue damage accumulation model under multiaxial variable amplitude loading, *International Journal of Mechanical Sciences*, 100, 180-194

5. Bu C.G., Sun L., Hu Y.B., Xia B.R., 2015, Research on flexible drill string vibration induced by sonic harmonic excitation, *Transactions of the Canadian Society for Mechanical Engineering*, **39**, 2, 281-291

6. Bu C.G., Tang X.Z., Wu W.G., 2022, A shallow subsurface magnetostrictive-driven sonic wave drill (in Chinese), Chinese Patent: CN202210343686.9

7. Bu C.G., Xiao J., He S.Y., Wiercigroch M., 2023, Theoretical study on fatigue damage of sonic standing wave resonant drill-string, *Journal of Petroleum Science and Engineering*, **220**, Part A, 111160

8. Chen H.X., Chen Y.X., Yang Y., 2014, A fatigue and low-energy shock-based approach to predict fatigue life, *Journal of Mechanical Science and Technology*, **28**, 10, 3977-3984

9. Fitzka M., Mayer H., 2016, Constant and variable amplitude fatigue testing of aluminum alloy 2024-T351 with ultrasonic and servo-hydraulic equipment, *International Journal of Fatigue*, **91**, Part 2, 363-372

10. Jiao R., He X.F., Li Y.H., 2018, Individual aircraft life monitoring: An engineering approach for fatigue damage evaluation, *Chinese Journal of Aeronautics*, **31**, 4, 727-739

11. Li C.C., Dong L.H., Wang H.D., Li G.L., Xu B.S., 2016, Metal magnetic memory technique used to predict the fatigue crack propagation behavior of 0.45%C steel, *Journal of Magnetism and Magnetic Materials*, **405**, 150-157

12. Li J.W., Zhong S., Lv G.P., Wang Z.G., Tian C., 2013, The variation of surface magnetic field induced by fatigue stress, *Journal of Nondestructive Evaluation*, **32**, 3, 238-241

13. Lin Y.H., Li G.H., Hu Q., Liu W.Y., 2015, Experimental study on drill pipe stress-fatigue life curve (in Chinese), *Petroleum Drilling Techniques*, **43**, 4, 124-128

14. Mayer H., Schuller R., Fitzka M., 2013, Fatigue of 2024-T351 aluminium alloy at different load ratios up to 10^{10} cycles, *International Journal of Fatigue*, **57**, 113-119

15. Miner M.A., 1945, Cumulative damage in fatigue, *Journal of Applied Mechanics*, **12**, 3, 159-164

16. Moradi S., Ranjbar K., 2009, Experimental and computational failure analysis of drillstrings, *Engineering Failure Analysis*, **16**, 3, 923-933

17. Rao J.S., Pathak A., Chawla A., 2001, Blade life: A comparison by cumulative damage theories, *Journal of Engineering for Gas Turbines and Power*, **123**, 4, 886-892

18. Sun L., Bu C.G., Hu P.D., Xia B.R., 2017, The transient impact of the resonant flexible drill string of a sonic drill on rock, *International Journal of Mechanical Sciences*, **122**, 29-36

19. Sun Q., Dui H.N., Fan X.L., 2014, A statistically consistent fatigue damage model based on Miner's rule, *International Journal of Fatigue*, **69**, 16-21

20. Wang Q., Lin Y.H., 2016, Effect of nitriding temperature on fatigue life of 4145 steel in QPQ salt bath composite heat treatment (in Chinese), *Technol. Innov. Appl.*, **33**, 23-24

21. Xiao J., Bu C.G., Hu Y.B., He S.Y., 2020, Influence of sonic vibrator mass on the modal frequency of the drill string, *Transactions of the Canadian Society for Mechanical Engineering*, **44**, 1, 65-71

22. Zamani S.M., Hassanzadeh-Tabrizi S.A., Sharifi H., 2016, Failure analysis of drill pipe: A review, *Engineering Failure Analysis*, **59**, 605-623

23. Zhao D., Hovda S., Sangesland S., 2018, Whirl simulation of drill collar and estimation of cumulative fatigue damage on drill-collar connection, *SPE Journal*, **23**, 2, 286-300

24. Zhu S.P., Huang H.Z., Liu Y., He L.P., Liao Q., 2012, A practical method for determining the Corten-Dolan exponent and its application to fatigue life prediction, *International Journal of Turbo and Jet Engines*, **29**, 2, 79-87

Manuscript received July 4, 2024; accepted for publication December 6, 2024